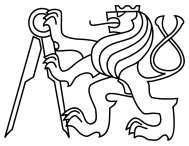

ČESKÉ VYSOKÉ UČENÍ TECHNICKÉ V PRAZE

PRÁCE PRO SOUTĚŽ O CENU AKADEMIKA BAŽANTA

Computer-Aided Plastic Limit Analysis of Plates

Autor:

Vladimír VANČÍK

Vedoucí práce:

Prof.Ing. Milan JIRÁSEK DrSc.

Abstract. This paper reports on a new tool for optimized design of reinforced concrete plates based on the yield line theory. The primary focus is on the development of a computer program which can analyze arbitrary yield line systems. The program includes a GUI for quick and intuitive input, and automatically performs analysis of yield line systems regardless of the complexity of their analytical solution. Furthermore, optimization of orthotropic reinforcement is implemented. Possible usage of the program for design compliant with Eurocode 2 is discussed.

Contents

1 Introduction **2**

2 Plastic limit analysis of plates **2**

2.1 Kirchhoff plate theory 2

2.2 Plastic limit analysis 4

2.2.1 The upper bound (kinematic) method 4

2.2.2 The lower bound (static) method 6

2.3 Definition of the ultimate plastic moment 6

3 Geometry of yield-line mechanisms **7**

3.1 Description of a yield-line mechanism as a system of equations 8

3.2 Process of solution 10

4 Description of the program **10**

4.1 Primary functionality - evaluation of limit loads 12

4.2 Secondary functionality - optimization 13

5 Ductility of collapse mechanisms **13**

5.1 Moment-curvature relation in a general cross section of an orthotropic plate . . 14

5.2 The method of ductility check 15

6 Comparison with FEM calculations **17**

7 Conclusion **20**

8 Acknowledgment **21**

1 Introduction

It has been shown e.g. in [1, 2] that design of reinforced concrete plates based on plastic limit analysis (specifically, on the yield-line theory) can lead to a significant reduction of reinforcement volume compared to the elastic design approach mostly employed in engineering practice. The yield-line theory corresponds to the kinematic method of limit analysis, which provides upper bounds on the limit load. It is therefore important to find the right collapse mechanism which minimizes the upper bound and leads to the actual limit load. The solution is also influenced by the ultimate bending moment which, for orthotropically reinforced concrete plates, can depend on the angle between the plate cross section (aligned with the yield-line) and the main reinforcement direction.

The search for the actual collapse mechanism has been extensively covered in [3, 4], but optimization of reinforcement proportion[1] has not received much attention. This paper describes the theoretical background and application of a new user friendly computer program for the analysis of yield-line mechanisms, allowing for both geometry and reinforcement optimization.

References [1, 2] offer an extensive validation of computations based on the yield-line theory by experiments. It is always assumed, however, that the plate is lightly reinforced and its ductility is sufficient. To check this assumption, we investigate whether some reasonable reinforcement ratios and proportions can lead to a situation in which the optimal collapse mechanism is not able to fully develop, due to limited ductility.

2 Plastic limit analysis of plates

2.1 Kirchhoff plate theory

Being itself a method of obtaining limit load, the yield-line theory needs an adequate description of plate behaviour. This is provided by the Kirchhoff plate theory. Its basic assumption says that normals to the plate center plane in its undeformed state remain straight and normal to it after deformation. As a result, there are no shear deformations, meaning only the moments contribute

[1] Assuming a plate reinforced in two mutually perpendicular directions, we will refer to the ratio of reinforcement area to concrete area in both directions as to the *reinforcement ratio*, as opposed to the ratio of the two reinforcement areas, which we will call the *reinforcement proportion*.

to the internal work, which is exactly what the yield-line theory needs. The Kirchhoff theory defines

$$u = -z\frac{\partial w}{\partial x} \tag{1}$$

$$v = -z\frac{\partial w}{\partial y} \tag{2}$$

with x, y being the in-plane coordinates, u, v the respective displacements, z the vertical coordinate with origin in the middle plane and w the deflection. The deformations are obtained as

$$\varepsilon_x = \frac{\partial u}{\partial x} = -z\frac{\partial^2 w}{\partial x^2} = z\kappa_x \tag{3}$$

$$\varepsilon_y = \frac{\partial v}{\partial y} = -z\frac{\partial^2 w}{\partial y^2} = z\kappa_y \tag{4}$$

$$\gamma_{xy} = \frac{\partial v}{\partial x} + \frac{\partial u}{\partial y} = -2z\frac{\partial^2 w}{\partial x \partial y} = z\kappa_{xy} \tag{5}$$

with κ_x, κ_y and κ_{xy} being the curvatures. The moments are obtained from stresses as

$$m_x = \int_{-\frac{h}{2}}^{\frac{h}{2}} z\sigma_x \mathrm{d}z \tag{6}$$

$$m_y = \int_{-\frac{h}{2}}^{\frac{h}{2}} z\sigma_y \mathrm{d}z \tag{7}$$

$$m_{xy} = \int_{-\frac{h}{2}}^{\frac{h}{2}} z\tau_{xy} \mathrm{d}z \tag{8}$$

As the plate theory assumes a state of plane stress, the virtual work of the inner forces is obtained accordingly as

$$W_{int} = \int_V (\sigma_x \delta\varepsilon_x + \sigma_y \delta\varepsilon_y + \tau_{xy}\delta\gamma_{xy})\mathrm{d}V \tag{9}$$

$$= \int_V (\sigma_x z\delta\kappa_x + \sigma_y z\delta\kappa_y + \tau_{xy} z\delta\kappa_{xy})\mathrm{d}V \tag{10}$$

Substituting $\mathrm{d}V = \mathrm{d}z\mathrm{d}A$, we obtain

$$W_{int} = \int_A \int_{\frac{-h}{2}}^{\frac{h}{2}} (\sigma_x z\delta\kappa_x + \sigma_y z\delta\kappa_y + \tau_{xy} z\delta\kappa_{xy})\mathrm{d}z\mathrm{d}A \tag{11}$$

and using (6), (7), (8) we arrive at the expression

$$W_{int} = \int_A (m_x \delta\kappa_x + m_y \delta\kappa_y + m_{xy} \delta\kappa_{xy}) \mathrm{d}A \tag{12}$$

which is ready for use in the yield-line theory as it contains only curvatures and moments.

2.2 Plastic limit analysis

The plastic limit analysis allows the redistribution of moments in a plate system, thus obtaining a greater limit load than with the elastic analysis. This becomes a reasonable approach for ductile materials, most importantly reinforced concrete or steel. Such materials are characterized by substantial deformation capacities after reaching their yield strength. For a plate under increasing static load the elastic limit state is reached as soon as the most highly stressed section reaches its yield moment. In reality, the load can increase beyond this limit. For sufficiently ductile materials, the deformation of the section can grow beyond the yield limit with only negligible moment increase, thus allowing the yielding to spread into other parts of the plate, forming a system of so-called yield hinges which represents the plastic limit state. Finding the right limit state for a given system is the objective of plastic limit analysis. Possible limit states can be examined by the upper bound or the lower bound method.

2.2.1 The upper bound (kinematic) method

The upper bound method for plates is called the yield-line theory and it is the basis of our program. It makes use of the balance of energy and gives an upper estimate of the limit load. To obtain the correct limit load, every possible kinematically admissible mechanism should be examined. Since examining one mechanism gives us one upper estimate of the limit load, the one that gives the lowest load is the correct one. A kinematically admissible mechanism is one that fulfills geometric boundary conditions and its external load power is positive. Furthermore it is assumed that the plastic deformations are concentrated in the yield lines and large enough to allow us to neglect the elastic deformations. That means that a fully developed yield-line mechanism will divide the plate into multiple planar segments with yield-lines acting as their axes of rotation. We can then obtain the limit load from the balance between dissipation rate in the yield lines and the external power. On the basis of Eq. (12), the dissipation rate can be

expressed in an orthogonal coordinate system ξ, η as

$$D_{int} = \int_A (m_\xi \dot{\kappa}_\xi + m_\eta \dot{\kappa}_\eta + m_{\xi\eta} \dot{\kappa}_{\xi\eta}) \mathrm{d}A \tag{13}$$

For a yield-line mechanism, this equation can be made much simpler. Let us examine the simple plate depicted in Fig. 1. Note that the axis ξ has been chosen as perpendicular to the yield line

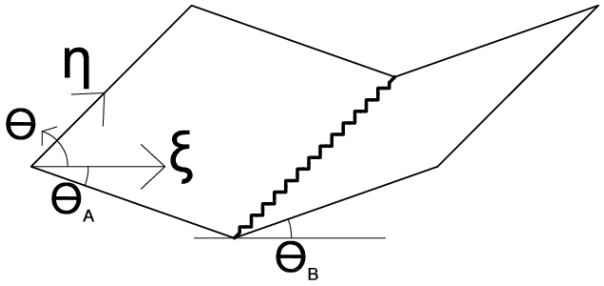

Figure 1: A simple one-way plate with one yield-line

in the center. Since the plate segments A and B are assumed to be planar, all of their curvatures will be zero. The only nonzero curvature rate in the yield-line is $\dot{\kappa}_\xi$. The limit plastic moment is achieved in the yield line, so $m_1 = m_{pl}$ will apply. Now we can write the dissipation rate for the one yield line as

$$D_{int,i} = \int_{\eta_1}^{\eta_2} \int_{\xi_l}^{\xi_r} m_{pl} \dot{\kappa}_\xi \mathrm{d}\xi \mathrm{d}\eta \tag{14}$$

with ξ_l and ξ_r being the coordinates just to the left and the right of the yield-line and η_1 and η_2 the coordinates of its begin and end along its length. Integration along the axes η, ξ leaves us with

$$D_{int,i} = (\eta_2 - \eta_1) m_{pl} \int_{\xi_l}^{\xi_r} \dot{\kappa}_\xi \mathrm{d}\xi = l m_{pl} (-\dot{\theta}_B - (-\dot{\theta}_A)) \tag{15}$$

so, finally, we have

$$D_{int,i} = l m_{pl} (\dot{\theta}_A - \dot{\theta}_B) \tag{16}$$

where l is the length of the yield-line and $\dot{\theta}_A$ and $\dot{\theta}_B$ the respective virtual plastic rotations of segments A and B. The rotations of a segment can be seen as vector quantities, so we can express the rotation difference with respect to a base orthogonal coordinate system x, y as the norm of the vector of rotation differences

$$\Delta\dot{\theta} = \dot{\theta}_A - \dot{\theta}_B = \sqrt{(\dot{\theta}_{x,A} - \dot{\theta}_{x,B})^2 + (\dot{\theta}_{y,A} - \dot{\theta}_{y,B})^2} \tag{17}$$

Now we can express the energy dissipation in a system of n yield-lines as

$$D_{diss} = \sum_{i=1}^{n} D_{diss,i} = \sum_{i=1}^{n} l_i m_{pl,i} \Delta\dot{\theta}_i \tag{18}$$

and then write the equation $D_{int} = P_{ext}$ as

$$\sum_{i=1}^{n} l_i m_{pl,i} \Delta\dot{\theta}_i = \int_A p(x,y)\dot{w}(x,y)\mathrm{d}A \tag{19}$$

For a uniformly loaded plate the function $p(x,y)$ becomes constant and the kinematically admissible load is then obtained as

$$p = \frac{1}{\int_A \dot{w}(x,y)\mathrm{d}A} \sum_{i=1}^{n} l_i m_{pl,i} \Delta\dot{\theta}_i = \frac{1}{\dot{V}} \sum_{i=1}^{n} l_i m_{pl,i} \Delta\dot{\theta}_i \tag{20}$$

where $\dot{V}$ denotes the rate of volume change. Alternatively, for a system of k force loads $P\lambda_i$

$$P = \frac{1}{\sum_{i=1}^{k} \lambda_i \dot{w}(x_i, y_i)} \sum_{i=1}^{n} l_i m_{pl,i} \Delta\dot{\theta}_i \tag{21}$$

2.2.2 The lower bound (static) method

The lower bound method gives a lower estimate of the limit load on the basis of equations of equilibrium. Accordingly, the mechanism that gives the largest limit load out of all the statically admissible mechanisms is the correct collapse mechanism. A statically admissible mechanism is characterized by a moment distribution such that:

1. The equations of equilibrium are fulfilled at every point.
2. The yield criterion is not exceeded anywhere.
3. The static boundary conditions are fulfilled.

An example of a lower bound method for plates is the strip method (see [2] for further details).

2.3 Definition of the ultimate plastic moment

The computation of the ultimate bending moment of a general reinforced concrete cross section has been addressed in many studies, looking, e.g., at the kinking of reinforcing bars. An extensive summary of the developments in this area can be found in [2], with the conclusion that the

Johansen yield criterion defined in [1] is accurate enough for the cases where in-plane normal forces are insignificant. According to Johansen, the ultimate bending moment on a yield-line (per unit length) is calculated as

$$M_{pl} = M_{pl,1} \sin^2 \phi + M_{pl,2} \cos^2 \phi \tag{22}$$

where

$$M_{pl,i} = N_i r_i \tag{23}$$

is the plastic moment for reinforcement direction number i and ϕ is the angle between the yield line and direcgtion 1; see Fig. 2. In Eq. (23),

$$N_i = h p_i f_y \tag{24}$$

is the normal force in the reinforcement per unit plate width (with h = height of the cross section, p_i = reinforcement ratio in direction i, f_y = yield strength of the reinforcement), and

$$r_i = h - d_{1,i} - \frac{a_i}{2} \tag{25}$$

is the lever of internal forces (with $d_{1,i}$ = distance of reinforcement from the cross section edge). The height of the compressive zone is calculated as

$$a_i = \frac{N_i}{f_c} \tag{26}$$

where f_c is the compressive strength of concrete.

Alternatively, the height of the compressive zone can be considered to be dependent on the angle ϕ, which gives slightly different results. Eq. (26) then reads

$$a = \frac{N_1 \sin^2 \phi + N_2 \cos^2 \phi}{f_c} \tag{27}$$

3 Geometry of yield-line mechanisms

Two basic theorems governing the development of yield-line mechanisms as stated in [1] are:

Theorem 1 *The yield line between two parts of a slab must pass through the point of intersection of their axes of rotation.*

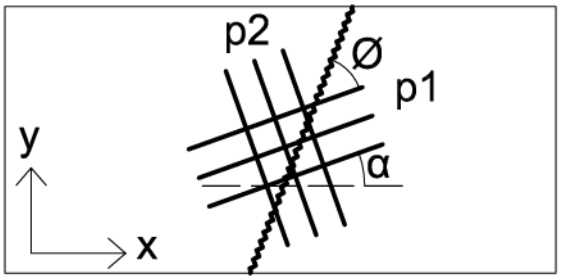

Figure 2: Reinforced plate: p_1 - reinforcement ratio in reinforcement direction 1, p_2 - reinforcement ratio in reinforcement direction 2 (perpendicular to direction 1), ϕ - the angle between direction 1 and the yield line

Theorem 2 *The yield pattern is determined by the axes of rotation of the various parts of the slab and the ratios between the rotations.*

These two theorems specify the conditions necessary to obtain a determined, geometrically compatible mechanism. This section contains a description of a system we devised to solve yield-line mechanisms. While we form its basic principles in a different way that is useful for code writing, their compliance with Theorem 1 will be remarked upon at a certain point where they are apparent.

3.1 Description of a yield-line mechanism as a system of equations

Geometrically, a general yield-line mechanism is defined through so-called 'plate segments' (henceforth refered to as 'segments'), which in turn are specified by nodes; see Fig. 3 with numbered nodes and segments. The segments represent rigid, mutually rotating parts of a yield-

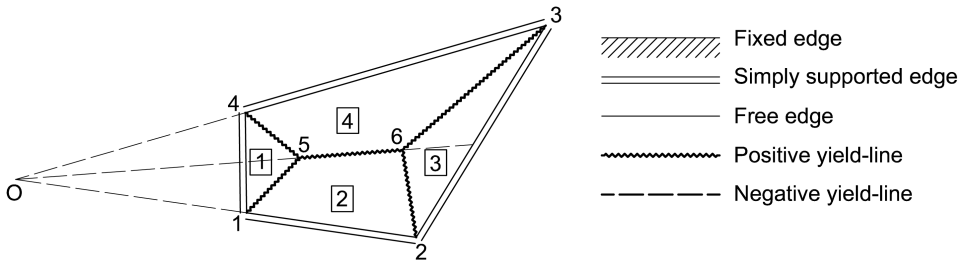

Figure 3: A yield-line mechanism for a general quadrilateral plate

line mechanism. They remain planar, which means that their deflection w is described by

$$w(x, y) = a + bx + cy \tag{28}$$

Thus, the motion of the segment is characterized by three parameters, a, b and c. Note that b and c have the meaning of segment rotations with respect to the coordinate axes and are later exploited when evaluating the kinematically admissible load from the equality of the external power and dissipation rate. Each segment is considered as a polygon with three or more vertices (nodes), each of which must displace according to (28).

Let us denote the number of segments n_s, the number of nodes defining a segment S_j, the number of nodes n_v and the number of segments sharing a node V_i. With that we define the total number of available equations

$$n_e = \sum_{i=1}^{n_v} V_i = \sum_{j=1}^{n_s} S_j \tag{29}$$

An equation

$$n_e = 3n_s + (n_v - n_0 - 1) + n_x \tag{30}$$

which represents the equality between the number of equations and the number of unknowns, must be satisfied. The term $3n_s$ accounts for the 3 unknown parameters of the plane equation of every segment. The term $(n_v - n_0 - 1)$ denotes the number of unknown deflections with n_0 being the number of supported nodes and the 1 being subtracted because a unit deflection will be prescribed in one of the unsupported nodes during the solution process. The remaining term n_x gives us information about the character of the mechanism in as much as:

1. When $n_x > 0$, the number of unknowns must be supplemented. To achieve that, n_x of the nodal coordinates of unsupported nodes have to pose as unknowns. We call those coordinates geometrically constrained. Their input value is be ignored and they are chosen during the solution as needed.

2. When $n_x = 0$, the solution is the simplest. All segment parameters can be directly obtained.

3. When $n_x < 0$, the mechanism has $(-n_x + 1)$ degrees of freedom which corresponds to an equivalent number of inner mechanisms, one of which will be critical.

3.2 Process of solution

The flowchart in Fig. 4 describes the most important steps of the solution. The first loop through plate segments ensures that we do not prescribe unit deflection in a supported node, i.e. it protects the solution against bad input.

An interesting step is the calculation of nodal variables(deflections and possibly coordinates) in the second loop. There are 4 different scenarios depending on the number of the node's adjoining segments with known parameters:

1. When parameters a, b, c of 1 segment are known, the deflection can be calculated from its equation using the node's prescribed coordinates.

2. When parameters a, b, c of 2 segments are known, the node must satisfy both their equations, so one of the spatial coordinates must be considered as an additional unknown. Its input value is overwritten by the solution.

3. When parameters a, b, c of 3 segments are known, both the spatial coordinates must be considered as additional unknowns so that all the segment equations may be fulfilled.

4. When parameters a, b, c of 4 or more segments are known, the node is over-determined and the solution fails.

The cases 2 and 3 are an illustrative example of the effect of Theorem 1. The choice of the unknown coordinate in case 2 is not always arbitrary – When the parameters of a node coordinate are equal in both segments, the node must lay on a line parallel to the respective coordinate axis. Thus, the other coordinate must be the unknown.

4 Description of the program

The program was developed in Python 2.7 environment using the Enthought TraitsUI package for the graphical interface (which is shown in Fig. 5). The code is object-oriented with emphasis on logical structure and extensibility. A class diagram is shown in Fig. 6 to aid the reader's orientation when we refer to specific objects later in the text.

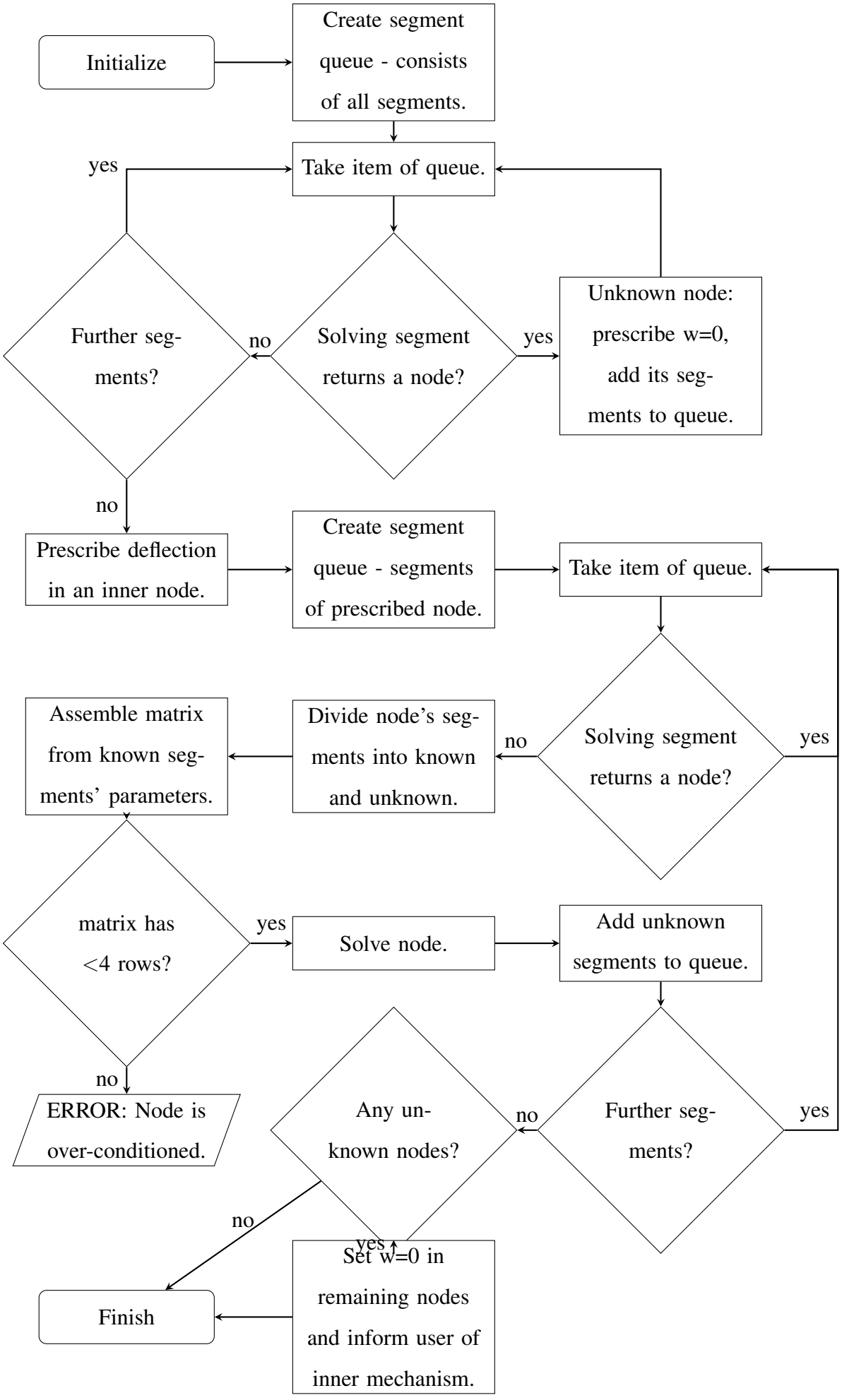

Figure 4: The solution of the geometry of a yield-line mechanism

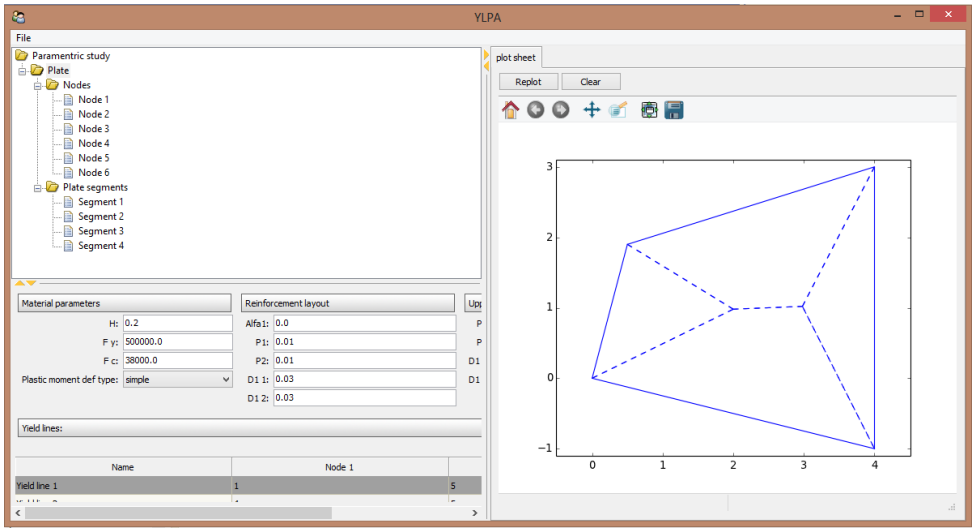

Figure 5: The user interface

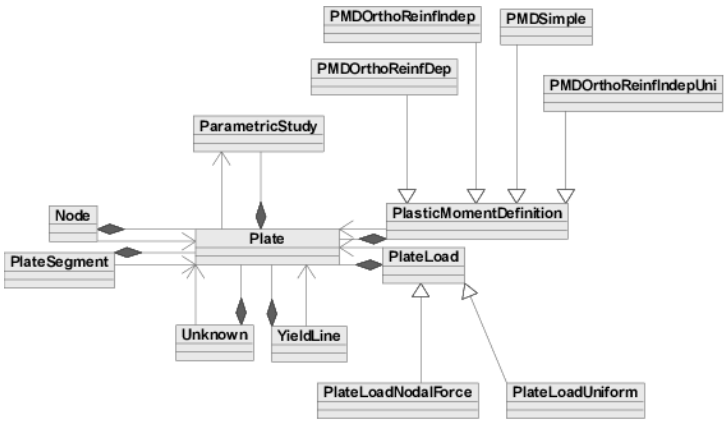

Figure 6: The class diagram

4.1 Primary functionality - evaluation of limit loads

The primary functionallity of the program is the evaluation of the limit load for yield-line mechanisms defined by the user. In order to do that, three separate tasks must be performed:

Obtaining a valid geometry, as has been extensively covered in section 3 is directed from the Plate object and accesses the PlateSegment and Node objects. The other two parts of the solution make use of the solved geometry.

Calculating the dissipation rate requires a material law, which is inherited from the parent class PlasticMomentDefinition. Various material laws are described in section 2.3.

Calculating the external power requires a definition of load, which is inherited from the parent class PlateLoad. Currently, force load and uniform load of the whole plate is possible. The limit load is obtained according to (21) and (20)

With such structure, all the maintenance and extension of the code can be performed separately for each of the three different tasks.

4.2 Secondary functionality - optimization

Another use case is the optimization of both the node coordinates and the plate parameters. Input data specific to optimization are managed by the ParametricStudy object, which containes a Plate object upon which the optimization is performed. The input data is divided into two categories - node data specify node coordinates and plate data specify plate attributes (in practice mostly reinforcement ratios, but any attribute may be chosen). Both data types then specify an optimization parameter on which they depend. That enables the user to set the conditions precisely and also save computation time, as more values can depend on one parameter (e.g. the two-way reinforcement of constant total volume). Optimization parameters are kept separately and may have their bounds specified. The limit load must be minimal over all admissible node positions but at the same time maximal with respect to plate attributes. The actual optimization is performed by the SciPy package optimize library - two function calls, one encapsulated in the other, are used to fulfill both the minimizing and the maximizing criteria.

5 Ductility of collapse mechanisms

As has been stated, we want to go beyond the simple assumption of lightly reinforced plates. Our program contains a routine for checking the rotational capacity of all yield lines. That allows us to easily detect cases where a seemingly optimal collapse mechanism cannot develop due to insufficient ductility.

5.1 Moment-curvature relation in a general cross section of an orthotropic plate

In order to propose a viable method for checking of the rotational capacity of a yield-line mechanism, we need to be able to obtain the yield and ultimate curvature of an arbitrary plate cross section. This can be done for cross sections of the main reinforcement directions in the same way as for a reinforced beam: take a cross section with yield strain in the reinforcement or ultimate strain in concrete and solve the balance of normal forces. For concrete, the stress-strain law for nonlinear calculations according to [6] should be utilized. However, in general, the reinforcement is not perpendicular to the cross section. To take that into account, we have to replace the general two-way reinforcement by an equivalent reinforcement which could be considered perpendicular to the cross section. The equivalent reinforcement should still provide an accurate bending moment, which is why we derive it from the equations for the ultimate plastic moment, as defined in section 2.3. First, we substitute N_i from (24) into (27) and obtain

$$a = \frac{h f_y (p_1 \sin^2 \phi + p_2 \cos^2 \phi)}{f_c} \tag{31}$$

This shows that the equivalent reinforcement ratio should be defined as

$$p_{eq} = p_1 \sin^2 \phi + p_2 \cos^2 \phi \tag{32}$$

Now, we substitute from (24) and (23) into (22) and write

$$M_{pl} = h f_y \Big[\Big(h - d_{1,1} - \frac{a}{2} \Big) p_1 \sin^2 \phi + \Big(h - d_{1,2} - \frac{a}{2} \Big) p_2 \cos^2 \phi \Big] \tag{33}$$

This can be rewritten as

$$M_{pl} = h f_y p_{eq} \Big(h - \frac{a}{2} - \frac{d_{1,1} p_1 \sin^2 \phi + d_{1,2} p_2 \cos^2 \phi}{p_{eq}} \Big) \tag{34}$$

which motivates the definition of the equivalent distance from the cross section edge

$$d_{1,eq} = \frac{d_{1,1} p_1 \sin^2 \phi + d_{1,2} p_2 \cos^2 \phi}{p_{eq}} \tag{35}$$

The values p_{eq} and $d_{1,eq}$ represent the reinforcement that would lead to the same bending moment if it were perpendicular to the cross section, as obtained from (22) with the height of the compressive zone given by (27). Using the equivalent reinforcement allows us to calculate the curvatures of any cross section of an orthotropically reinforced plate. Though the proposed method has not been verified experimentally, we believe it can provide sensible results.

5.2 The method of ductility check

So far, we have described how we obtain the curvatures for a general cross section. We shall denote the yield curvature as κ_y and the ultimate curvature as κ_u. For a plate with multiple yield lines we have to calculate κ_y and κ_u for each yield line. It is convenient to arrange the values κ_u into a diagonal matrix – let us denote it as $\mathbf{K}_u$. Another vector, denoted as $\vec{r}$, will be formed by the relative rotations of segments adjacent to the yield lines. From the vector $\vec{r}$ we derive a matrix of scaled rotations $\mathbf{R}$ with components

$$R_{i,j} = \frac{r_j}{r_i} \tag{36}$$

and the control product

$$\mathbf{P} = \mathbf{K}_u\mathbf{R} \tag{37}$$

A row in the matrix $\mathbf{P}$ represents the real curvatures in the respective yield lines when the yield line corresponding to that row reaches its ultimate curvature. If at least one row has all its values within the bounds of the respective κ_y and κ_u, the ductility of the system is sufficient.

Arguably, only the yield moment should be used as the limit plastic moment in order to be on the safe side, because the described method only guarantees that every yield line has reached at least its yield curvature. However, the yield and ultimate moment obtained from the curvature calculations with the nonlinear stress-strain diagram for concrete are very close to the moment obtained by Johansen's yield criterion with constant stress in concrete. Following this, we always use the Johansen's yield criterion as it is much faster. The curvature calculations are used solely for the purpose of the ductility check.

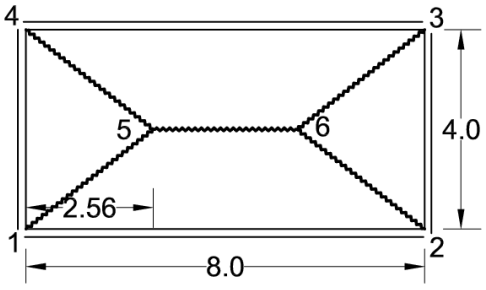

Figure 7: A plate with an optimized yield-line pattern for $p_1 = p_2 = 0.02$, $d_{1,1} = 0.04\ m$, $d_{1,2} = 0.035\ m$, $h = 0.15$ m.

Having performed the ductility check on a few examples we find that it is actually quite hard

to find a plate where the insufficient ductility poses an issue. The rectangular plate depicted in Fig. 7 has been optimized for a very high reinforcement ratio of 0.02 in both directions. As we can see from the results of the ductility check in Tab. 1 (particularly the third line of the control product $\mathbf{P}$), the ductility of the plate is insufficient, though very narrowly. If we reduce the

yield-line	1-5	4-5	6-5	2-6	3-6
$\mathbf{R}$	1.000	1.000	1.575	1.000	1.000
	1.000	1.000	1.575	1.000	1.000
	0.635	0.635	1.000	0.635	0.635
	1.000	1.000	1.575	1.000	1.000
	1.000	1.000	1.575	1.000	1.000
κ_y	0.0439	0.0439	0.0427	0.0439	0.0439
$\mathbf{P}$	0.0663	0.0663	0.104	0.0663	0.0663
	0.0663	0.0663	0.104	0.0663	0.0663
	0.0421	0.0421	0.0663	0.0421	0.0421
	0.0663	0.0663	0.104	0.0663	0.0663
	0.0663	0.0663	0.104	0.0663	0.0663
κ_u	0.0663	0.0663	0.0663	0.0663	0.0663

Table 1: The results of the ductility check of the plate from Fig. 7.

longitudinal reinforcement $p_{1,1}$ to 0.017, the ductility becomes sufficient, with y_5 diminishing from 2.56 m to 2.43 m and y_6 acting symmetrically. This is caused partly by the reduction of the yield curvature κ_y of the corner yield lines and partly by the diminishing ratio between the rotations in yield line 5-6 and the other yield lines. This tendency remains unchanged with further diminishing p_1. Theoretically, if p_1 could go all the way down to zero, it would at some point reach a value $p_{1,t}$ at which the ratio between the yield line rotations becomes equal to the ratio between the ultimate curvatures. From $p_1 = p_2$ up to $p_1 = p_{1,t}$, the actual failure would start in yield line 5-6, and with further diminishing p_1 it would start in the corner yield lines. $p_1 = p_{1,t}$ is therefore the case when the failure begins everywhere at once and it is therefore safe to use the ultimate bending moment as the limit plastic moment. However, as was already mentioned, the difference between the yield and the ultimate bending moments is

minute. Moreover, the building codes specify that the main reinforcement in plates must be supplemented by perpendicular reinforcement of at least 20% of their volume, which is still much more than the value of $p_{1,t}$ in this case.

It should be brought to attention, that the proposed method of ductility check ceases to provide sensible results when the so-called fan mechanisms are examined - those are used to approximate circular yield lines e.g. in the corners of plates with fixed edges (see Fig. 8). The relative rotation in a radial yield-line of the fan mechanism gets smaller with refinement of the mechanism while rotations not in the fan mechanism remain the same. Thus, for a fine enough fan mechanism, the proposed method would eventually report insufficient ductility. However, such densely concentrated yield-lines as in the fan mechanism can no more be considered to achieve the plastic moment separately, but rather the whole mechanism should be taken as a smeared plastic zone.

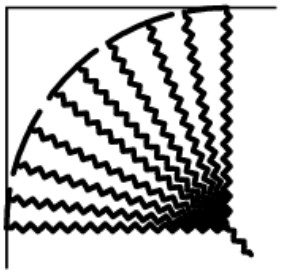

Figure 8: A corner fan mechanism

6 Comparison with FEM calculations

This section shows a comparison of results obtained by our program and by the finite element code OOFEM (see [8]). As an example we chose a rectangular plate from an ideally elasto-plastic material simply supported on all sides, loaded by uniform load or central force. The size of the plate is 6x4 m, thickness 0.15 m. The plastic material is characterized by the Mises yield criterion, the corresponding material model in OOFEM being 'MisesMat'. The yield strength has been chosen as $f_y = 200$ MPa, the Poisson ratio $\nu = 0.3$, and Young's modulus $E = 210$ GPa, which more or less corresponds to steel.

As the material is isotropic, we can perform the calculations with our program for unit mo-

ment and multiply the results with the actual ultimate moment. The ultimate stress will be obtained from the Mises yield criterion for the state of plane stress expressed with the principal stresses

$$\sigma_1^2 - \sigma_1\sigma_2 + \sigma_2^2 = 3\tau_0^2 \tag{38}$$

Since there is no shear stress between plate segments, one of the principal axes in a yield line will be aligned with its direction (let us say axis 1). Thus, we seek the ultimate stress perpendicular to that direction – the stress σ_2. Because the plate's deformation rate along a yield line must be zero, the normal to the Mises yield surface in the point where it is reached will be parallel to axis 2 (). Taking the derivative of (38) with respect to σ_1 we obtain

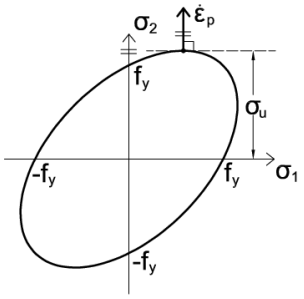

Figure 9: A section of the Mises yield surface corresponding to the state of plane stress

$$2\sigma_1 - \sigma_2 = 0 \tag{39}$$

and substituting $\sigma_1 = \frac{\sigma_2}{2}$ into (38) we get the ultimate stress

$$\sigma_u = \sigma_2 = 2\tau_0 \tag{40}$$

To express the ultimate stress in terms of our input values we need to examine the state of uniaxial stress. Substituting $\sigma_1 = f_y, \sigma_2 = 0$ we obtain from (38)

$$\tau_0 = \frac{f_y}{\sqrt{3}} \tag{41}$$

which when substituted into (40) yields

$$\sigma_u = \frac{2}{\sqrt{3}} f_y \tag{42}$$

and with the above stated value of $f_y = 200$ MPa we have $\sigma_u = 230.9$ MPa.

The unit plastic moment reads

$$m_{pl} = \sigma_u \left(\frac{h}{2}\right)^2 \tag{43}$$

and with $h = 0.15$ m we obtain $m_{pl} = 1.30$ MNm/m.

Since the problem is symmetrical, we model only one fourth of the plate in OOFEM in order to save computation time. The element size is 4x4x1.875 cm which corresponds to 75 elements for the longer side, 50 for the shorter side and 8 for the height. In total that makes 30000 elements and 34884 nodes. As there is reason to expect volumetric locking, elements based on the B-bar formulation have been used alongside standard 8-node linear spatial elements.

The resulting load curves for the case of uniform load are shown in Fig. 10a. We can observe the expected overestimation of the load by the standard linear elements. This is further illustrated by Fig. 12b, in which we can see that the first derivative of the load curve for the standard elements converges to a positive value as opposed to the B-bar elements whose load curve seems to converge to zero. Fig. 10b shows the plastic deformations on a deformed plate. The resulting plastic zone is in good agreement with the yield-line solution. Though the yield-line solution gives a slightly higher limit load, this can be attributed to the fact that the solution with 3d elements allows a more general failure mechanism to develop as it is not governed by the Kirchhoff plate theory.

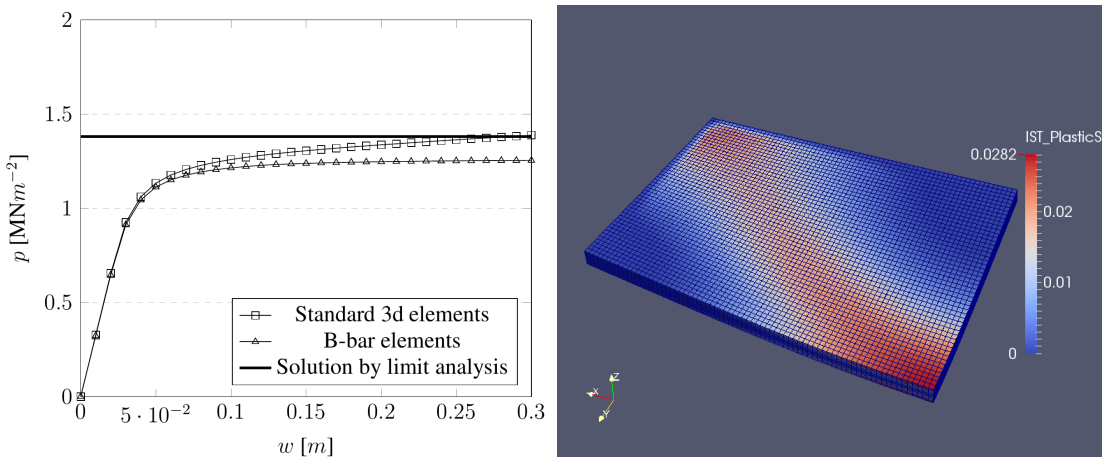

(a) Load curve (b) Plastic deformations

Figure 10: Results for a plate under uniform load

The resulting load curves for the case of central force load are shown in Fig. 11a. Again, we can observe the locking of the standard elements, with the derivatives plotted in Fig 12a.

The difference between the FEM solution and the yield-line theory is here slightly greater than in the previous case. While the point made about the difference of the theories obviously still applies, a further issue is that we have not reached a very good plastic zone(see Fig. 11b) even though the solution is controlled by displacement of the center node while a patch of 5x5 nodes in the center is loaded by force load.

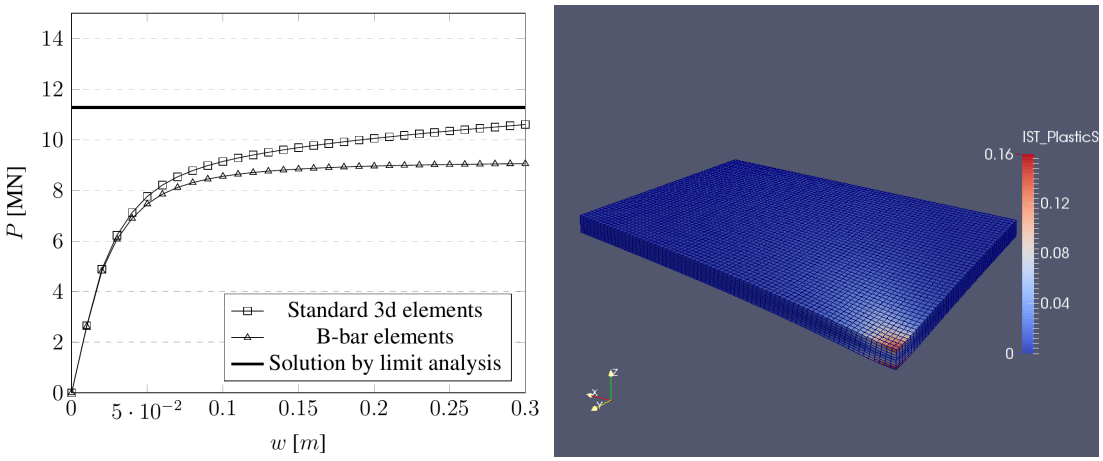

(a) Load curve (b) Plastic deformations

Figure 11: Results for a plate under force load

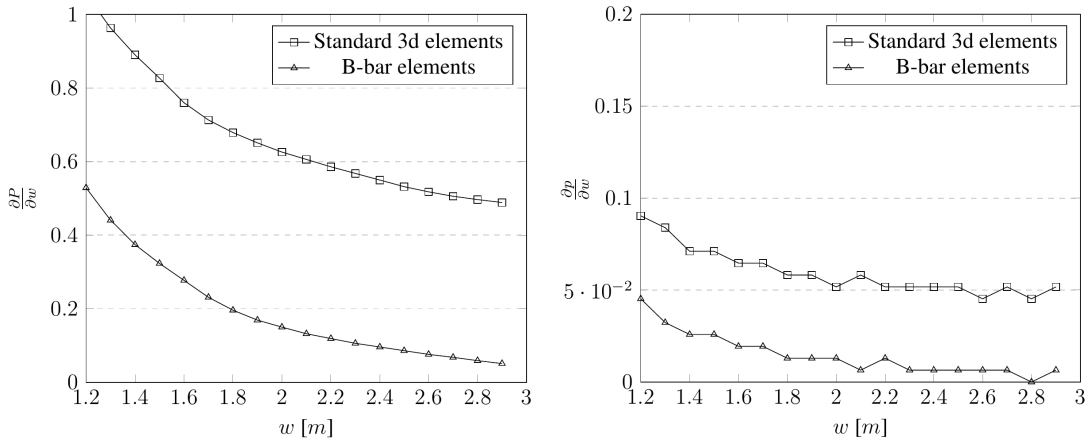

(a) Force load (b) Uniform load

Figure 12: Derivatives of the load curves

7 Conclusion

The main objective – the development of a computer program – has been achieved. The reliability of the results has been verified by comparison with various analytical solutions found in [1, 7]. The author believes that the code is very readable and easily extensible and will be pleased to provide it upon request. The simple GUI has potential as an interactive educational tool.

A possible method of checking the ductility of collapse mechanisms has been proposed. We have verified on an example that the assumption of sufficient ductility of orthotropically reinforced plates is greatly justified.

Comparative computations with the finite element method have been performed for a plate from an ideally elasto-plastic material, finding good compliance with results by the yield-line theory.

Among future objectives are the implementation of a material law which considers compression in the reinforcement and some studies of rectangular plates reinforced at both surfaces. Furthermore, the comparison with results from OOFEM is to be extended by a reinforced concrete plate.

8 Acknowledgment

Financial support received from the Grant Agency of the Czech Technical University in Prague under SGS project No. 15/031/OHK1/1T/11 is gratefully acknowledged.

References

[1] K. W. Johansen: Yield-line Theory, Cement and Concrete Association, 1962

[2] R. Park, W. L. Gamble: Reinforced Concrete Slabs, John Wiley & Sons, 1980

[3] A. Thavalingam, A. Jennings, J. J. McKeown, D. Sloan: A computerised method for rigid-plastic yield-line analysis of slabs, Computers and Structures 68 (1998) 601–612

[4] A. Thavalingam, A. Jennings, D. Sloan, J. J. McKeown: Computer-assisted generation of yield-line patterns for uniformly loaded isotropic slabs using an optimisation strategy, Engineering Structures 21 (1999) 488–496

[5] A. Jennings: On the identification of yield-line collapse mechanisms, Engineering Structures 18 (1996) 332-337

[6] EN 1992-1-1:2004 + AC:2010, (CEN, 2010)

[7] Z. Sobotka: Teorie plasticity desek, Academia, 1973

[8] B. Patzák. OOFEM - an object-oriented simulation tool for advanced modeling of materials and structures. Acta Polytechnica, 52(6):59–66, 2012.